Latin American Journal of Solids and Structures
www.lajss.org

Damage Identification from Uniform Load Surface Using Continuous and Stationary Wavelet Transforms

Abstract

Derived from flexibility matrix, Uniform Load Surface (ULS) is used to identify damages in beam-type structures. This method is beneficial in terms of more participating the lower order modes and having less prone to noise and irregularities in the measured data in comparison with the original flexibility matrix technique. Therefore, these characteristics make this approach a practical tool in the field of damage identification. This paper presents a procedure to employ stationary wavelet transform multi-resolution analysis (SWT-MRA) to refine ULS obtained from the damaged structure and then using continuous wavelet transform (CWT) for localizing the discontinuity of improved ULS as a sign of damage site. Evaluation of the proposed method is carried out by examining a cantilever beam as a numerical case, where the ULS is formed by using mode shapes of damaged beam and two kinds of wavelets (i.e. *symmetrical 4* and *bior 6.8*) is applied for discerning the induced crack. Moreover, a laboratory test is conducted on a free-free beam to experimentally evaluate the practicability of the technique.

Keywords

Modal analysis, damage detection, wavelet analysis, flexibility matrix, uniform load surface

M. Masoumi, M. R. Ashory*

Modal Analysis Laboratory, School of Mechanical Engineering, Semnan University, P. O. Box 35195-363, Semnan, Iran

Received in 21 Sep 2012
In revised form 02 Aug 2013

*Author email:
mashoori@semnan.ac.ir

1 BACKGROUND

The wide assortment of efforts has been dedicated to assess the influence of damages on dynamic behavior of structures with the aim of proposing new techniques to localize flaws and cracks (Farrar and Worden, 2007; Alvandi and Cremona, 2006; Yan et al, 2007; Morassi and Vestroni, 2008; Farrar et al, 2001). Two fundamental dynamic properties including natural frequencies and mode shapes have gained more attention in the field of damage identification through modal analysis. Based on different numerical methods and state of the art signal processing techniques, different

procedures have been introduced. Up to now, fractal dimension (FD) and generalized fractal dimension (GFD) technique, gapped smoothing method (GSM), strain energy method (SEM), differential quadrature method (DQM), global fitting method (GFM), and applying the discrete and continuous wavelet transforms to the mode shapes (Ratcliffe , 1997; Liew and Wang, 1998; Hong et al, 2002; Hadjileontiadis et al, 2005; Hadjileontiadis and E. Douka, 2007; Wang and Qiao, 2007; Qiao et al, 2007; Yoon et al, 2005, 2010), flexibility matrix or uniform load surface (ULS) (Qiao et al, 2007; Bakhshizade et al, 2011; Masoumi and Ashory, 2012) have been used.

A fractal dimension-based crack detector (FDCD) was put forward by Hadjileontiadis et al (Hadjileontiadis et al, 2005; Hadjileontiadis and E. Douka, 2007). They proved that since fractal dimension is able to measure the complexity of a signal, it can be used as a damage detector due to the fact that any crack in structure results in more complex vibrational signal. So as to improve some shortcoming of the FD method in specific situations, Wang and Qiao (Wang and Qiao, 2007) recommended GFD and modified FD by adding a scale parameter. SEM was firstly proposed by Stubbs et al (Stubbs et al, 1992) where their formulations were rooted in the strain energy of a Bernoulli-Euler beam and needed to have access to both mode shapes of intact and damaged structure. This technique was also used for plate-type structures by Cornwell et al (Cornwell et al, 1999). Bakhshizade et al (Bakhshizade et al, 2011) originally used DQM to evaluate a damaged beam and successfully localized the crack. GSM was brought into play by Ratcliffe (Ratcliffe, 1997) where he used a modified Laplacian operator to identify small damages from the fundamental mode shape of the damaged structure. GFM, which is an extended technique based on GSM, was developed by Yoon et al (Yoon et al, 2005, 2010) to detect damage in both beam- and plate-type structures.

Granted Liew and Wang (Liew and Wang, 1998) firstly used spatial discrete wavelet transform (DWT) to examine a numerical model of a simply supported damaged beam, but their method was in need of an oscillating excitation along the length of the beam. Wang and Deng (Wang and Deng, 1999) carried out an investigation on the use of DWT in vibration based damage detection. Their technique was based on applying Haar DWT to the measured displacement, strain or acceleration. Hong et al (Hong et al, 2002) studied the use of Mexican hat continuous wavelet transform (CWT) with the aim of finding damage in a numerically modeled beam. Cao and Qiao (Cao and Qiao, 2008) proposed a method to have synergistic advantages of stationary wavelet transform (SWT) and CWT simultaneously. Their method includes implementing SWT Multiresolution analysis (SWT-MRA) to refine the obtained mode shapes of a damaged beam and then looking for damage site through applying CWT to the refined mode shapes.

Using flexibility matrix was firstly proposed by Pandey and Biswas (Pandey and Biswas, 1994). They defined a vector formed by the absolute difference between the flexibility matrix of intact and damaged state of a beam. As an attempt to improve the method, Zhang and Aktan (Zhang and Aktan, 1998) used uniform load surface (ULS) and showed that this new approach is more capable in comparison to traditional flexibility technique. They also performed experimental tests on a highway bridge. Wu and Law (Wu and Law, 2004) applied ULS to the mode shapes of a plate and numerically studied the effects of various boundary conditions, noise levels and sensor spacing.

In this paper, a new approach is used based on three major steps. First, extracted mode shapes of damaged beam are employed to form ULS and then SWT-MRA is used to improve the obtained ULS and eliminate the irregularities and noises. Finally, the location of the induced crack is detected by using CWT multiscale analysis.

2 FUNDAMENTAL THEORIES

2.1 Wavelet Theories

CWT of a space domain signal is given by

$$CW(\tau,s)=\int_{-\infty}^{\infty} f(x)\psi^{*}{}_{\tau,s}(x)\,dx=\left\langle \psi_{\tau,s}(x),f(x)\right\rangle \tag{1}$$

where $\psi^{*}(x)$ is the complex conjugate of the mother wavelet. The mother wavelet is defined as

$$\psi_{\tau,s}(x)=\frac{1}{\sqrt{a}}\psi\left(\frac{x-s}{\tau}\right) \tag{2}$$

in which, τ,s are translation and scale parameters respectively ($\tau,s\in\Re,\tau>0$). When the designated scale is large, global view of the signal is provided and when small-scale is selected, a detailed view of the signal is given. Any function can be chosen as the mother wavelet if it satisfies the following admissibility condition

$$\int_{-\infty}^{\infty}\frac{\left|\Psi(\omega)\right|^{2}}{\omega}d\omega<\infty \tag{3}$$

Here, $\Psi(\omega)$ is the Fourier transform of $\psi(x)$. Choosing the different mother wavelets provides various wavelet transforms. In this work, *symmetrical 4* and *bior 6.8* are selected as wavelet functions to identify damages in a beam structure.

Although CWT has been extensively used in the field of damage detection, it has some incapability in the face of noisy data. To overcome this weakness, SWT is used to de-noise the obtained data before applying CWT to find damage location. SWT is similar to DWT except that the number of wavelet coefficients at each level remains equal to the number of sampling points of the original signal while using DWT results in reduction of the number of coefficients by $N/2^{L}$, where N is the number of sampling points of the original signal and L stands for L^{th} decomposition level (Cao and Qiao, 2008). To obtain DWT formulation, scale and translation parameters of CWT are considered on a discrete space which results in a discrete set of continuous

basis functions. By setting $\tau = \xi_0^j, s = k\xi_0^j\zeta_0$ in which $\xi_0 > 1$ is a dilated step and $\zeta_0 \neq 0$ is a translation step, the family of wavelets is given by

$$\psi_{j,k}(x) = \xi_0^{-j/2}\psi(\xi_0^{-j}x - k\zeta_0) \tag{4}$$

and DWT of a given signal f(x) is defined as

$$DW(j,k) = \int_{-\infty}^{\infty} \psi_{j,k}^*(x) f(x) = \left\langle \psi_{j,k}(x), f(x) \right\rangle \tag{5}$$

As Cao and Qiao mentioned (Cao and Qiao, 2008), DWT has a significant drawback in comparison to SWT. Although DWT can decompose a multicomponent signal into a group of component signals and remove unnecessary components, shift variance characteristic causes inaccurate outcomes in damage location procedure. This problem is especially noticeable when the sampling points are not close to each other and the measured data is not a high-resolution signal. It is worth mentioning that in this work, spline interpolation is utilized to increase the number of data points and provide smooth data, which is used as an input signal for wavelet analysis.

2.2 ULS Theory

Modal flexibility matrix for a system with m measured modes is approximately given by

$$F_m \approx \sum_{r=1}^{m} \frac{\phi_r \phi_r^T}{\omega_r^2} \tag{6}$$

By defining the deflection vector under uniform load for a system with n degrees of freedom

$$\eta_{j,k} = \begin{bmatrix} f_{1,1} & f_{1,2} & \cdots & f_{1,n} \\ f_{2,1} & f_{2,2} & \cdots & f_{2,n} \\ \vdots & \vdots & \vdots & \vdots \\ f_{n,1} & f_{n,2} & \cdots & f_{n,n} \end{bmatrix} \begin{Bmatrix} 1 \\ 1 \\ \vdots \\ 1 \end{Bmatrix} \tag{7}$$

ULS is obtained as:

$$u(j) = \sum_{k=1}^{n} \eta_{j,k} = \sum_{k=1}^{n} \left(\sum_{r=1}^{m} \frac{\phi_r^j \phi_r^k}{\omega_r^2} \right) = \sum_{r=1}^{m} \frac{\phi_r^j \sum_{k=1}^{n} \phi_r^k}{\omega_r^2} \tag{8}$$

where ϕ_r is the rth mode shape of damaged structure and ω_r stands for the rth natural frequency. $f_{i,j}$ is the modal flexibility at the point i under the unit load at the point j. As Zhang and Aktan (Zhang and Aktan, 1998) maintained, the inverse of the square of the frequency leads to the less contribution of higher order modes in comparison to the flexibility matrix and truncation error, stemmed from using lower order modes, can be small for a system with well-separated frequencies. In the flexibility matrix based damage detection techniques, if either deflection location and load location or one of them is placed at the boundaries, an error may cause due to the high noise to signal ratio. They observed that ULS is less error-sensitive than the original modal flexibility.

3 DISCUSSION ABOUT THE CHOICE OF WAVELET

Over the almost twenty years of using wavelet transform for damage identification many different wavelet transforms have been used and their efficiency has been evaluated for numerical and experimental cases. Ovanesova and Suarez (Ovanesova and Suarez, 2004) showed that *Morlet*, *Mexican Hat*, *Gaussian* and *Shannon* wavelets are not suitable to use as DWT due to the lack of the scaling function. In addition, different authors have used various wavelets such as *Symlets* (Khatam et al, 2007), *Coiflets* (Carrión et al 2006; Rucka and Wilde, 2006), *biorthogonal* (Cao and Qiao, 2008; Ovanesova and Suarez, 2004; Prasad et al 2006; Masoumi and Ashory, 2012), *Daubechies* (Hou et al, 2000) and *symmetrical* (Douka et al, 2003). Although a high number of vanishing moments leads to better outcomes, increasing the vanishing moments needs to provide longer support because a wavelet holding n vanishing moments should have at least $2n-1$ support length (Hong et al, 2002). In this paper two mother wavelets called *symmetrical 4* and *biorthogonal*, mentioned by previous authors as efficient and practical in damage detection of beam type structures (Cao and Qiao, 2008; Ovanesova and Suarez, 2004; Prasad et al 2006; Masoumi and Ashory, 2012; Douka et al, 2003), are used.

4 NUMERICAL CASE STUDY

A cantilever beam, as a numerical case, is considered so as to investigate the proposed method. Its properties are as follows: width of 0.045 m, height of 0.012 m, length of 1 m, Young's Modulus of 200 Gpa, and density of $\rho = 7850\,{kg}/{m^3}$. The number of elements of FE model is fifty and they have equal lengths. Nine damage scenarios are induced based on Table 1, in which a is the depth of the damage.

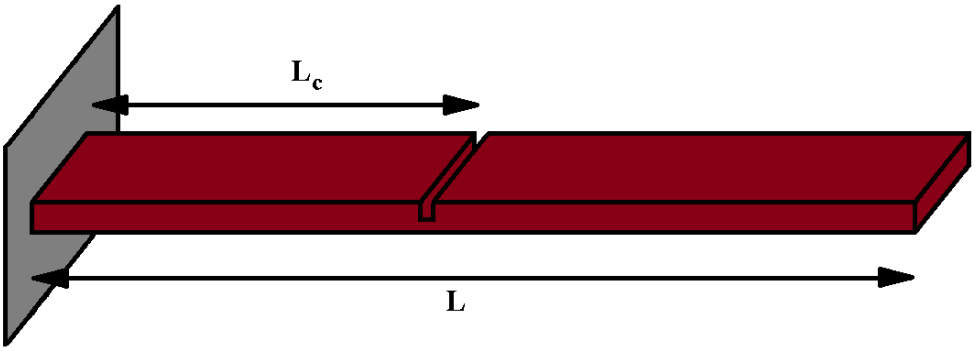

Figure 1 Layout of the damaged beam

Table 1 Damage Scenarios

	Location (L_c) mm	Severity (a/h) %		Location (L_c) mm	Severity (a/h) %		Location (L_c) mm	Severity (a/h) %
Case I	100	10	Case IV	100	25	Case VII	100	40
Case II	500	10	Case V	500	25	Case VIII	500	40
Case III	900	10	Case VI	900	25	Case IX	900	40

Table 2 shows the first six natural frequencies before and after inducing damage on the beam. As expected, an increase in damage severity results in decreasing the natural frequencies. For cases close to the free-end, first natural frequency is unchanged while higher order natural frequencies provide more tangible variations. One can conclude that the prediction of damage size based on only variation of frequencies of damaged beam and having no information from its FE model is not feasible owing to the fact that a decrease in frequencies ensuing from damage is contingent on damage site.

Table 2 Comparison of natural frequencies for nine damage scenarios

Natural Frequency (Hz)	Intact beam	Case I	Case II	Case III	Case IV	Case V	Case VI	Case VII	Case VIII	Case IX
First	9.78	9.75	9.78	9.78	9.50	9.73	9.78	9.32	9.70	9.78
Second	61.32	61.25	61.16	61.31	60.78	60.08	61.29	60.44	59.28	61.27
Third	171.69	171.67	171.69	171.63	171.52	171.68	171.18	171.41	171.67	170.81
Fourth	336.45	336.41	335.59	336.11	336.16	330.00	333.69	335.96	326.00	331.72
Fifth	556.18	555.75	556.14	555.14	552.86	555.89	547.89	550.73	555.70	542.14
Sixth	830.85	829.49	828.77	828.67	820.72	815.78	814.15	814.40	806.90	803.43

ULSs were formed using eq. (8) for each case. Not only maximum wavelet coefficients of *symmetrical 4* CWT and *bior6.8* CWT but also all of the coefficients, before and after refining the ULSs by utilizing SWT, were obtained and tabulated in Table 3, Table 4 and graphically depicted in Figures 3-11.

As presented in Table 3 and Table 4, although there is no damage in the intact state of the beam, the maximum wavelet coefficient is almost equal to the coefficient obtained for case III where 10 percent damage was induced at 100 mm from free-end of the beam. This problem stems from irregularities in wavelet coefficients at the free-end boundary and it has been undermined by refining the data by using SWT before implementing *symmetrical 4* CWT. Generally, wavelet coefficients are decreased due to the use of SWT to refine the vibration data, but this issue is worth dealing because of the compensation received from this technique where a noticeable reduced amount of unfavorable abnormalities is seen in the results.

Table 3 Maximum wavelet coefficients for symmetrical 4 and the corresponding locations

Damage Case	Max Wavelet Coefficients for CWT (x10^{-7})	Location (mm)	Max Wavelet Coefficients for SWT+CWT (x10^{-7})	Location (mm)
Intact	1.81	900	0.063	938
Case I	12.83	104.7	6.21	95.3
Case II	3.55	536.4	2.04	475.4
Case III	1.84	923.4	0.13	921.1
Case IV	104.17	104.7	49.27	95.3
Case V	32.95	484.8	16.16	475.4
Case VI	2.55	935.2	0.9	876.5
Case VII	177.17	104.7	83.68	95.3
Case VIII	56.95	484.75	27.46	475.4
Case IX	3.15	935.2	1.54	876.5

Table 4 Maximum wavelet coefficients for bior6.8 and the corresponding location

Damage Case	Max Wavelet Coefficients for CWT (x10^{-7})	Location (mm)	Max Wavelet Coefficients for SWT+CWT (x10^{-7})	Location (mm)
Intact	0.96	945	0.048	937.5
Case I	10.91	109.3	6.22	100
Case II	3.55	489.4	2.04	480
Case III	1.03	937.5	0.12	878.9
Case IV	86.38	109.4	49.36	100
Case V	28.2	489.4	16.2	480
Case VI	1.66	940	0.92	878.9
Case VII	146.7	109.4	83.84	100
Case VIII	47.93	489.4	27.52	480
Case IX	2.66	888.3	1.56	878.9

Inaccuracy in damage localization by utilizing CWT and SWT+CWT techniques for both wavelet transforms have been provided in Figure 2, where the error of each approach is presented. When the induced damage is at the location close to the clamped-end, the use of *bior6.8* CWT provides us with the maximum value of error in the results whereas the use of SWT in association with *bior6.8* CWT leads to a completely accurate localization procedure, containing no error. At these locations, i.e. close to the clamped-end, error in localization for *symmetrical 4* CWT is equal to the error obtained through employing SWT in conjunction with *symmetrical 4* CWT. When the crack is in the middle of the beam, *bior6.8* CWT has the minimum error and an increase in damage severity results in a decrease in estimated error of damage localization for *symmetrical 4* CWT approach while the error in other three approaches remains consistent.

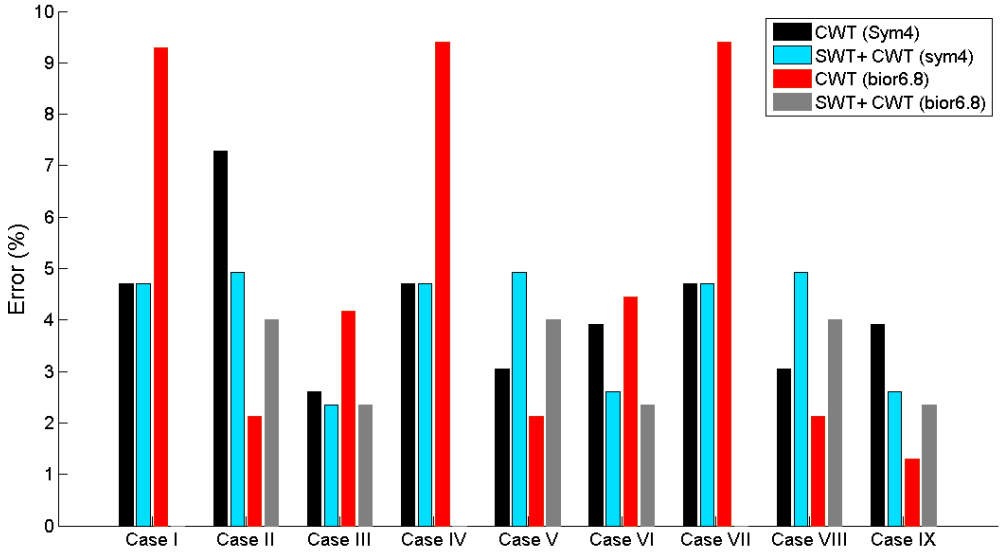

Figure 2 Error in damage localization before and after using SWT

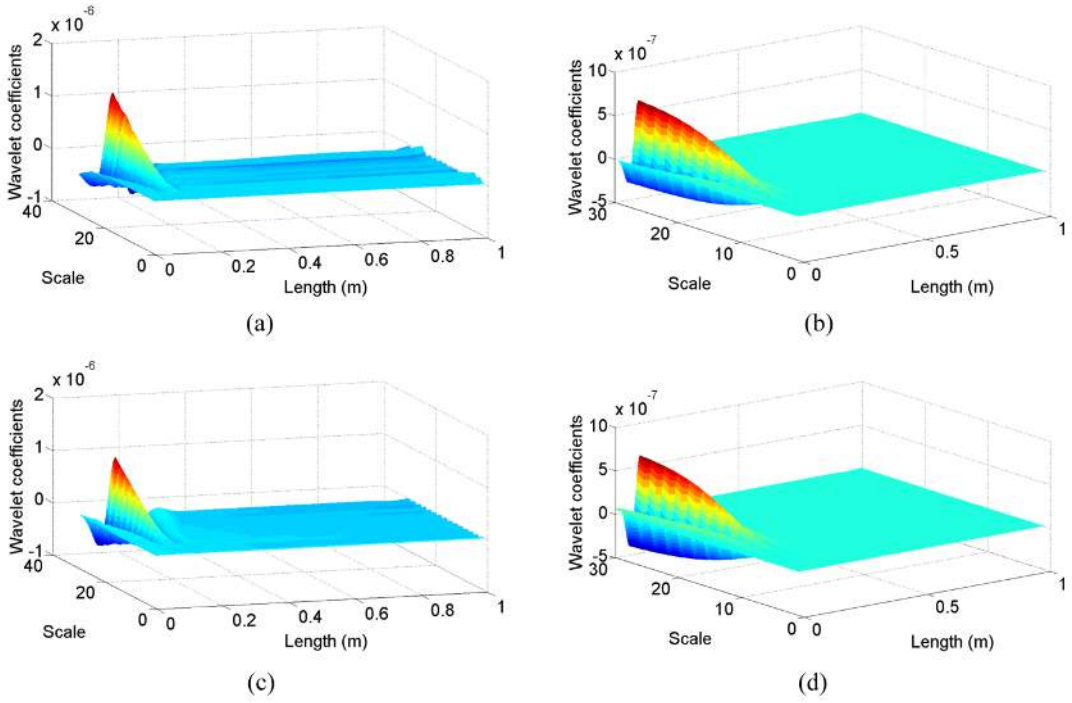

Figure 3 Wavelet coefficients for Case I: (a) symmetrical 4 CWT, (b) SWT+ symmetrical 4 CWT, (c) bior6.8 CWT, (d) SWT+ bior6.8 CWT

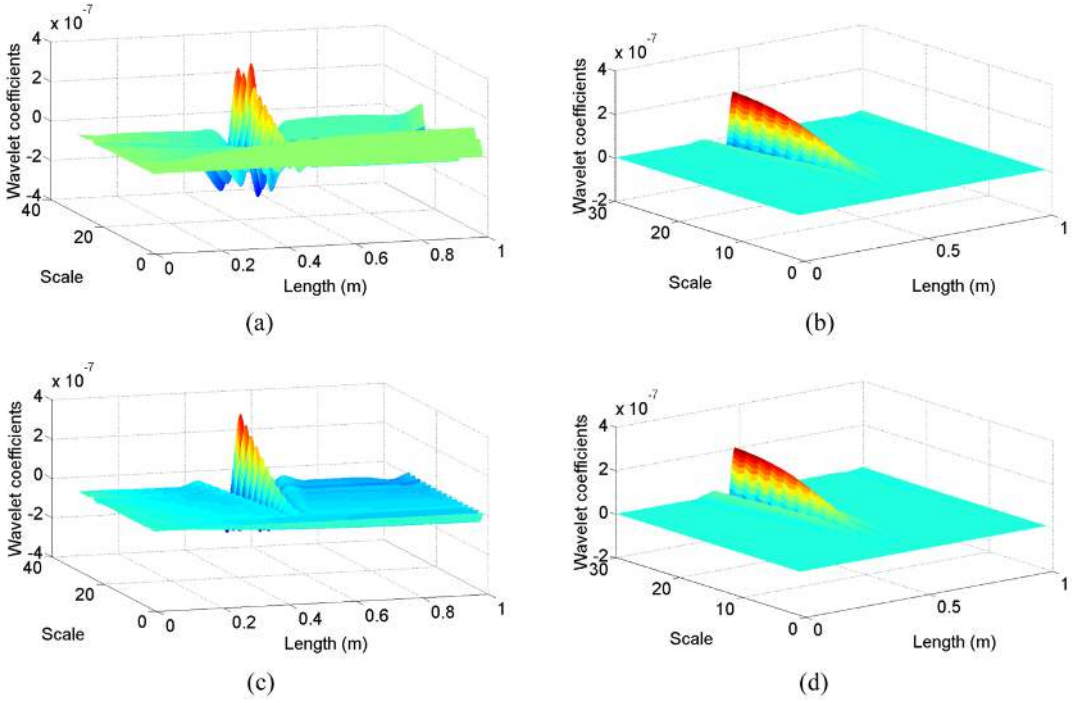

Figure 4 Wavelet coefficients for Case II: (a) symmetrical 4 CWT, (b) SWT+ symmetrical 4 CWT, (c) bior6.8 CWT, (d) SWT+ bior6.8 CWT

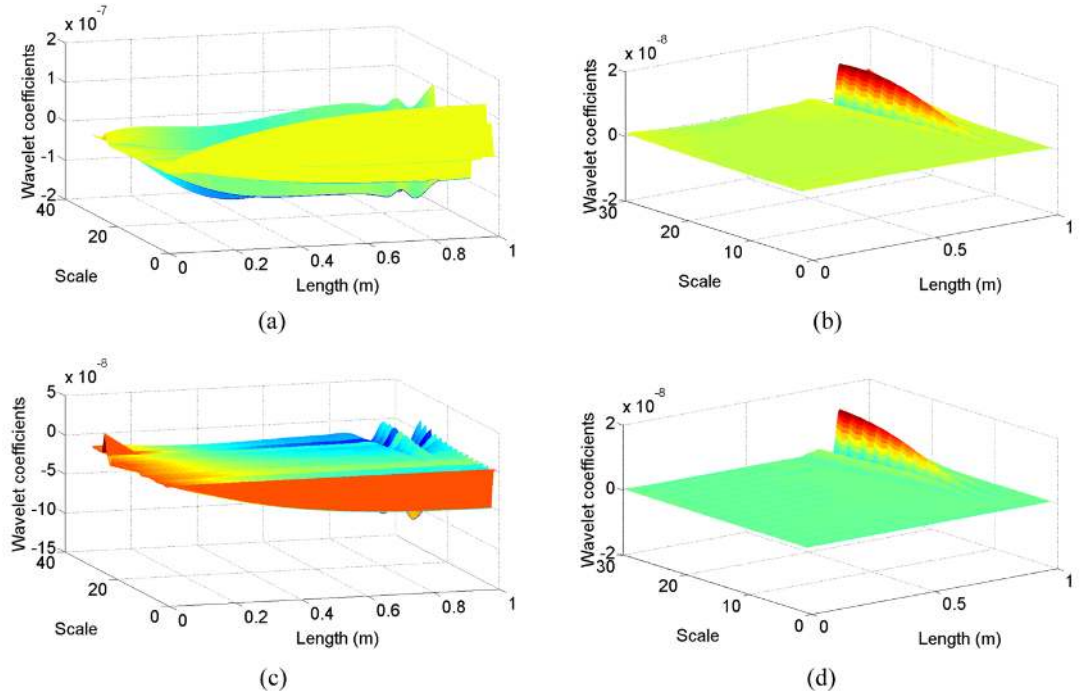

Figure 5 Wavelet coefficients for Case III: (a) symmetrical 4 CWT, (b) SWT+ symmetrical 4 CWT, (c) bior6.8 CWT, (d) SWT+ bior6.8 CWT

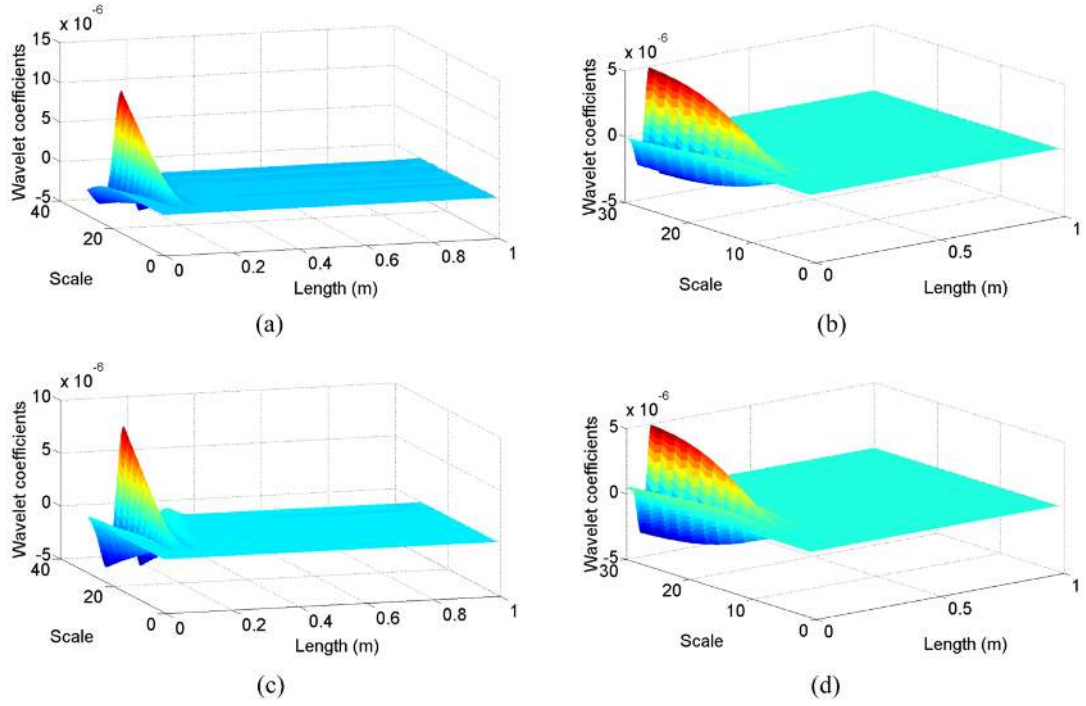

Figure 6 Wavelet coefficients for Case IV: (a) symmetrical 4 CWT, (b) SWT+ symmetrical 4 CWT, (c) bior6.8 CWT, (d) SWT+ bior6.8 CWT

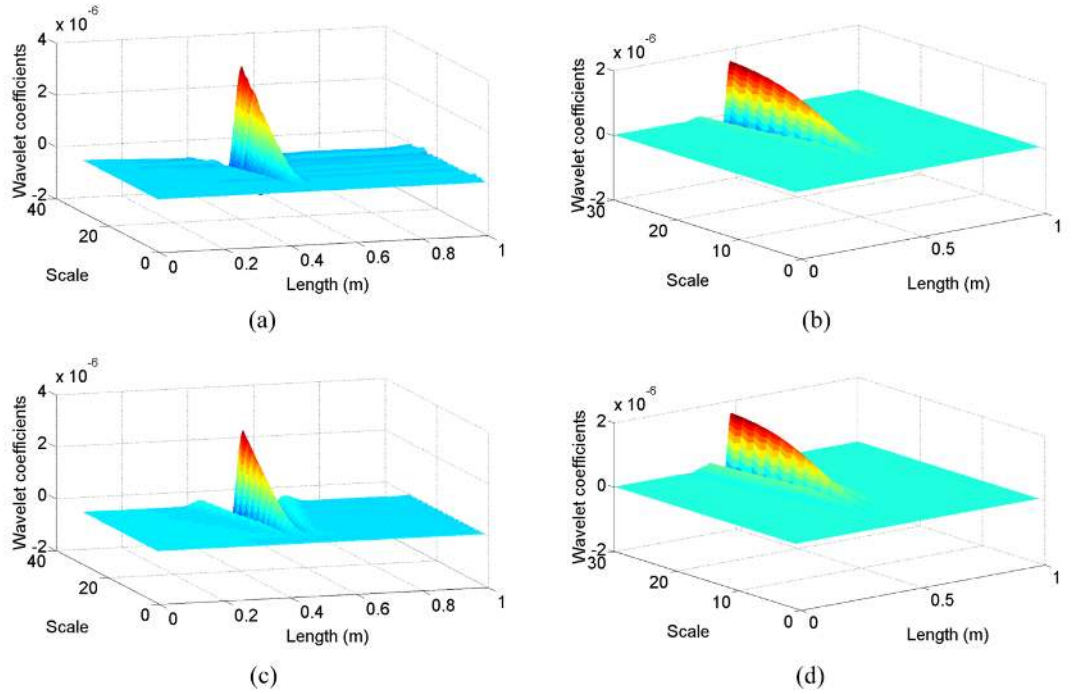

Figure 7 Wavelet coefficients for Case V: (a) symmetrical 4 CWT, (b) SWT+ symmetrical 4 CWT, (c) bior6.8 CWT, (d) SWT+ bior6.8 CWT

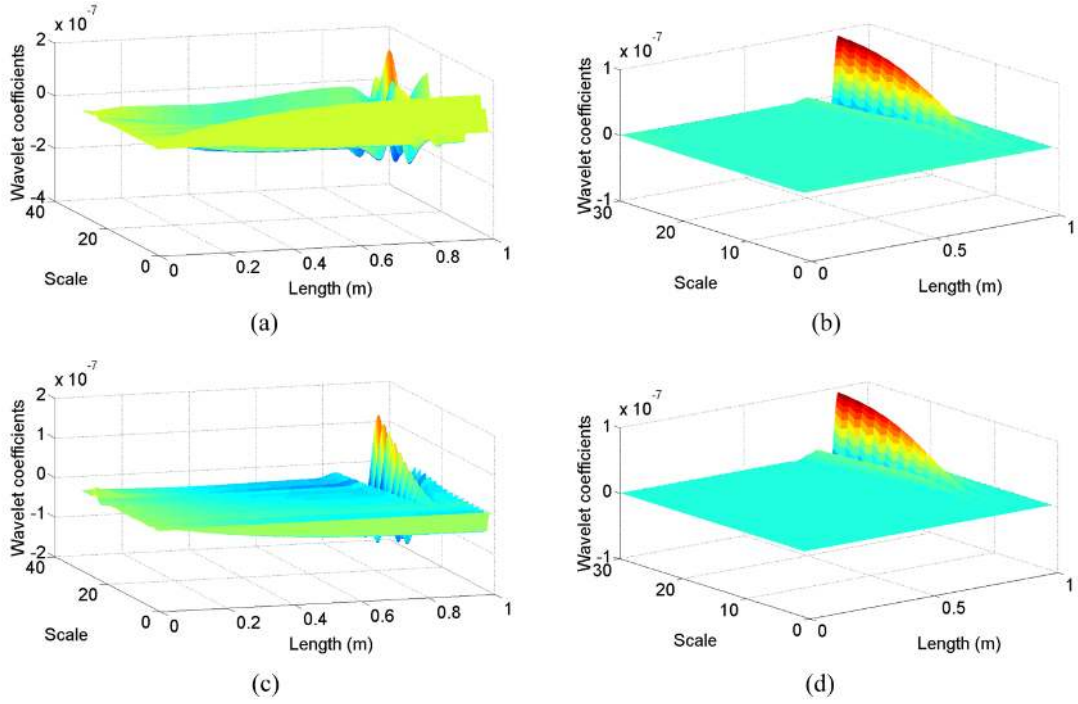

Figure 8 Wavelet coefficients for Case VI: (a) symmetrical 4 CWT, (b) SWT+ symmetrical 4 CWT, (c) bior6.8 CWT, (d) SWT+ bior6.8 CWT

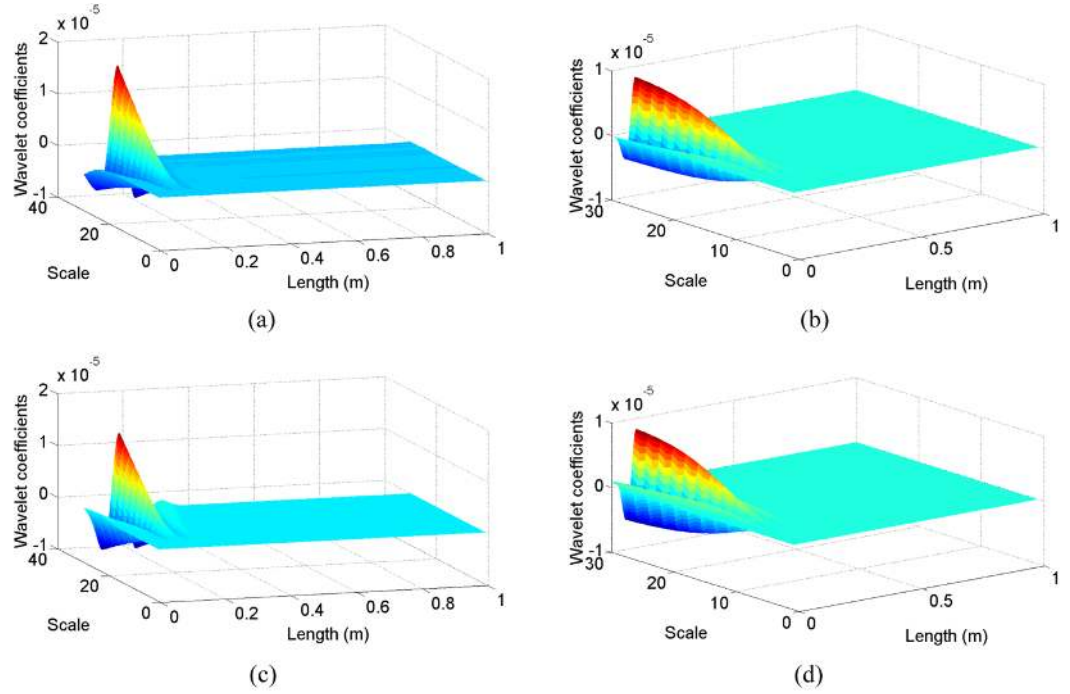

Figure 9 Wavelet coefficients for Case VII: (a) symmetrical 4 CWT, (b) SWT+ symmetrical 4 CWT, (c) bior6.8 CWT, (d) SWT+ bior6.8 CWT

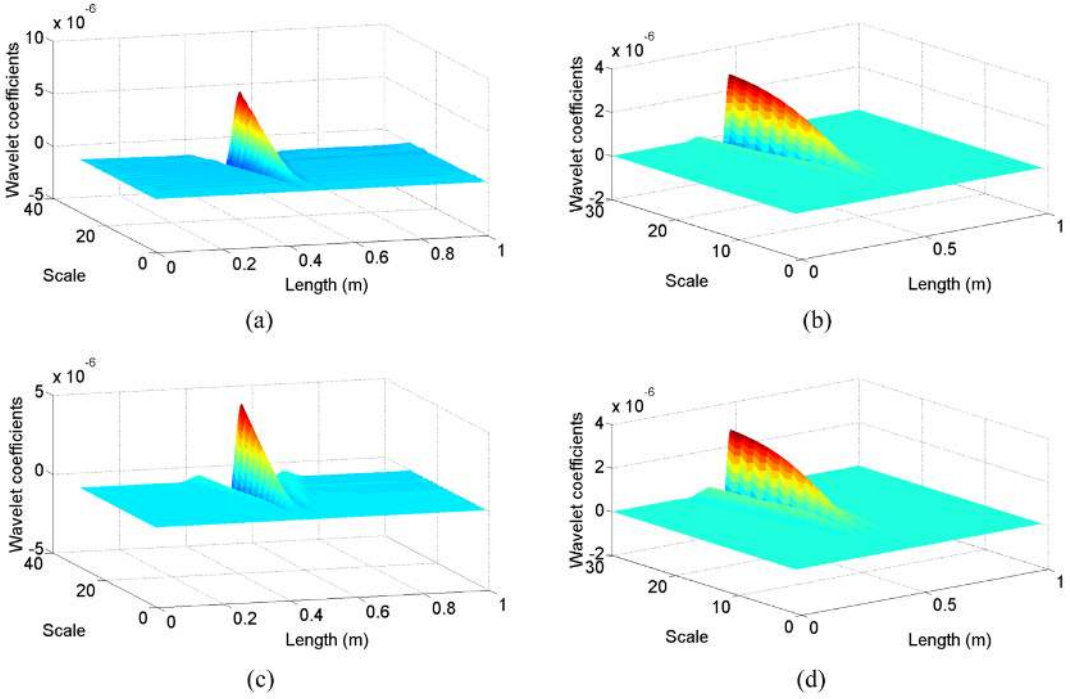

Figure 10 Wavelet coefficients for Case VIII: (a) symmetrical 4 CWT, (b) SWT+ symmetrical 4 CWT, (c) bior6.8 CWT, (d) SWT+ bior6.8 CWT

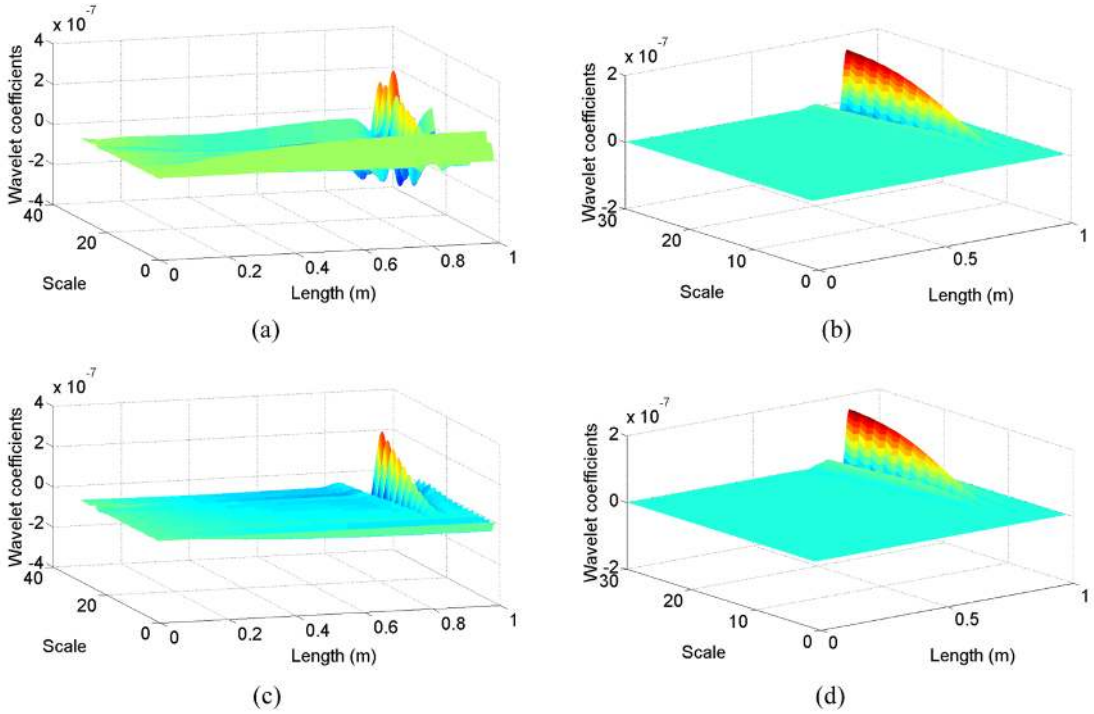

Figure 11 Wavelet coefficients for Case IX: (a) symmetrical 4 CWT, (b) SWT+ symmetrical 4 CWT, (c) bior6.8 CWT, (d) SWT+ bior6.8 CWT

Figures 3-11 show the wavelet coefficients for all damage scenarios, which are described in Table 1. In all cases, using SWT to refine the data before applying CWTs has almost eliminated the unfavorable irregularities in the results. These figures indicate that locating damage close to the free-end causes more irregularities even though this effect decreases with increasing the damage severity. Moreover, they confirm the results provided in Table 3 and 4 showing that an increase in damage size brings about an increase in wavelet coefficients at the crack site and also coefficients are larger for *symmetrical 4* CWT compared to *bior6.8* CWT. The privilege of using the SWT_MRA is more noticeable when the crack is located close to the free-end where before refining the data by using SWT, it is challenging to discern the location of crack especially for *symmetrical 4* CWT.

5 EXPERIMENTAL CASE STUDY

To experimentally establish the feasibility of the proposed technique for identifying damage in structures, a 0.94 m length beam with a cross-section of 0.05 x 0.01 m was tested. A 30% Damage was induced at 0.51 m from one end of the beam and an accelerometer was placed on 0.48 m. In the conducted hammer test, force and response signals were measured by using PULSE software and mode shapes were obtained by ICATS software. The test setup configuration for the hammer test of the free-free beam and measured Frequency Response Functions (FRFs) along with the

obtained first four mode shapes are shown in Figure 12. As shown, no sign of damage is noticed in the obtained mode shapes without using signal processing techniques.

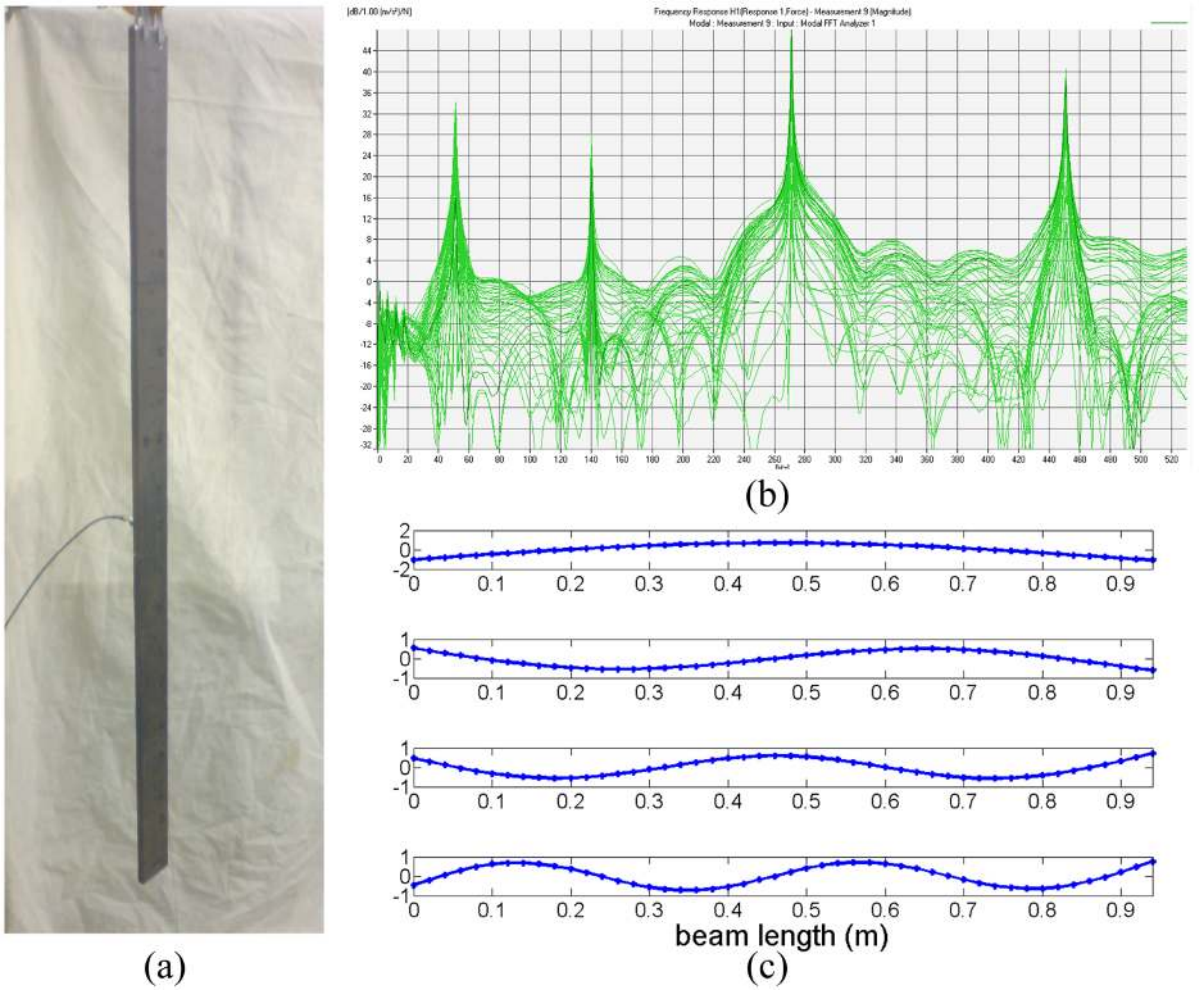

Figure 12 (a) hammer test setup configuration (b) 46 measured FRFs (c) First four mode shapes of free-free damaged beam

Eq. (8) was used to form ULS and then spline interpolation and extrapolation were utilized to smooth the interior and boundary points of the formed ULS. At the first step, *symmetrical 4* and *bior 6.8* were employed to find the damage site. Results are shown in Figure 13 (a) and (c). Even though the damage site is detectable, there are irregularities especially at the boundaries. In order to de-noise the results and achieve outcomes with less irregularity, SWT_MRA was firstly used to refine the ULS of damaged beam and then wavelet coefficients of *symmetrical 4* and *bior6.8* were calculated. This is shown in Figure 13 (b) and (d) for two aforementioned wavelets.

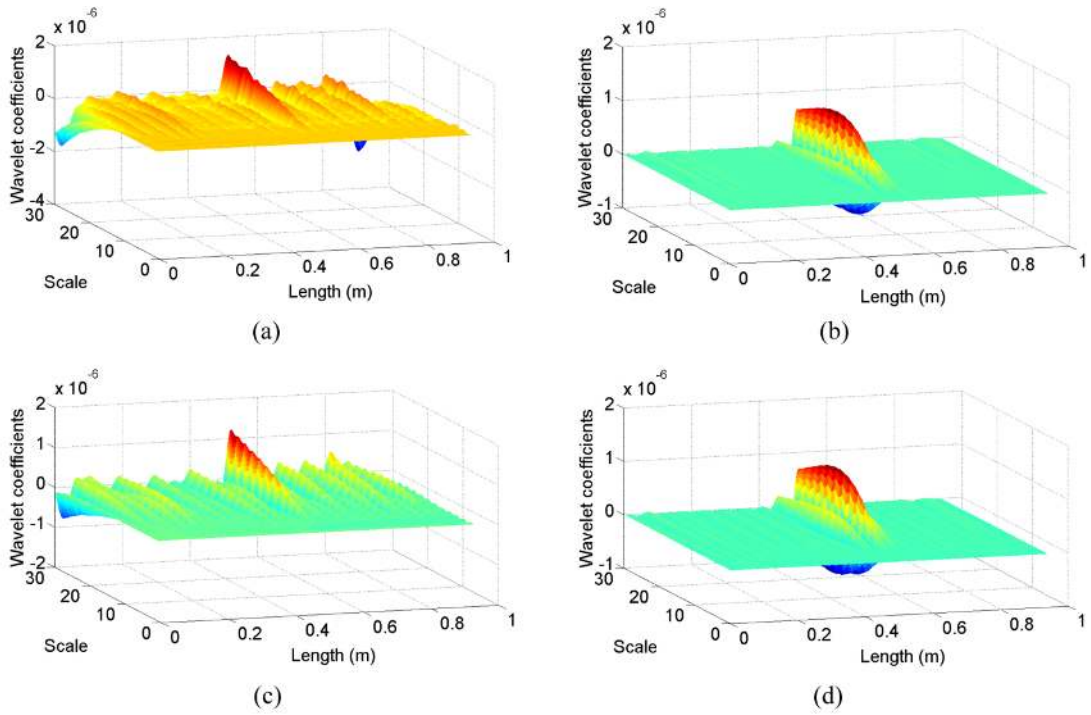

Figure 13 Wavelet coefficients for experimental case: (a) symmetrical 4 CWT, (b) SWT+ symmetrical 4 CWT, (c) bior6.8 CWT, (d) SWT+ bior6.8 CWT

It can be seen that the wavelet coefficients at damage location are decreased compared to using CWT but most of the abnormalities in the coefficients are eliminated. The only point that should be noticed in the experimental case is that increasing the scale parameter for this approach is not a route to provide better results and as it shown in this case, there is a specific suitable range of scales for aptly finding the crack.

6 SUMMARY AND CONCLUSIONS

An approach for identifying damage in structures was proposed, where ULS of damaged structure was firstly refined by applying the SWT-MRA and then crack site was discerned by using CWT multiscale analysis. Proposed approach was numerically and experimentally investigated by a cantilever and a free-free beam respectively. Two kinds of continuous wavelets were applied to the ULS namely *symmetrical 4* and *bar 6.8*. Equipped with the privilege of having less prone to noise and irregularities in the data, the new technique seemed to provide more accurate outcomes in damage detection procedures through wavelet based signal processing. For a cantilever beam, numerical studies revealed that damages located close to the free-end of the beam are more difficult to find when SWT-MRA is not implemented. The only drawback that happens is that SWT-MRA generally decreases the values of obtained wavelet coefficients.

Acknowledgements This work is supported by the Talented Office of Semnan University.

References

Alvandi A. and Cremona C. Assessment of vibration-based damage identification techniques. Journal of Sound and Vibration, 292(1-2): 179–202, 2006.

Bakhshizade A., Ashory M. R., Masoumi M. and Salmani A. non model-based damage detection method using generalized flexibility matrix. International Operational Modal Analysis Conference, Istanbul, Turkey, 2011.

Cao M. and Qiao P. Integrated wavelet transform and its application to vibration mode shapes for the damage detection of beam-type structures. Smart Mater. Struct., 17(5): 1–17, 2008.

Carrión F., Lozano A. and Castaño V. Condition monitoring of vibrating steel-reinforced concrete beams through wavelet transforms. Structural Survey, 24(2): 154-162, 2006.

Cornwell P., Doebling S. W., and Farrar C. R. Application of the strain energy damage detection method to plate-like structures. Journal of Sound and Vibration, 224(2): 359-374, 1999.

Douka E., Loutridis S. and Trochidis A. Crack identification in beams using wavelet analysis. International Journal of Solids and Structures, 40(13-14): 3557–3569, 2003.

Farrar C. R. and Worden K. An introduction to structural health monitoring. Phil. Trans. R. Soc., 365(1851):303-315, 2007.

Farrar C. R., Doebling S. W., and Nix D. A. Vibration–based structural damage identification. Phil. Trans. R. Soc., 359(1778): 131-149, 2001.

Hadjileontiadis L. J. and Douka E. Crack detection in plates using fractal dimension, Engineering Structures, 29(7): 1612–1625, 2007.

Hadjileontiadis L. J., Douka E., and Trochidis A. Fractal dimension analysis for crack identification in beam structures. Mechanical Systems and Signal Processing, 19(3): 659–674, 2005.

Hong J. C., Kim Y. Y., Lee H. C., and Lee Y. W. Damage detection using the Lipschitz exponent estimated by the wavelet transform: applications to vibration modes of a beam. International Journal of Solids and Structures, 39(7): 1803–1816, 2002.

Hou Z., Noori M. and Amand R.S. Wavelet-based approach for structural damage detection. Journal of Engineering Mechanics, 126(7): 677-683, 2000.

Khatam H., Golafshani A.A., Beheshti-Aval S. and Noori M. Harmonic class loading for damage identification in beams using wavelet analysis. Structural Health Monitoring, 6(1): 67-80, 2007.

Liew K. M. and Wang Q. Application of wavelet theory for crack identification in structures. Journal of Engineering Mechanics, 124(2): 152-158, 1998.

Masoumi M. and Ashory M. R. Damage localization by wavelet analysis of uniform load surface. Journal of Vibroengineering, 14(1): 395-407, 2012.

Morassi A. and Vestroni F. Dynamics Methods for Damage Detection in Structures. SpringerWienNewYork, 2008.

Ovanesova A. and Suarez L. Applications of wavelet transforms to damage detection in frame structures. Engineering Structures, 26(1): 39-49, 2004.

Pandey A. K. and Biswas M. Damage detection in structures using changes in flexibility. Journal of Sound

and Vibration, 169(1): 3-17, 1994.

Prasad B.K.R., Lakshmanan N., Muthumani K. and Gopalakrishnan N. Enhancement of damage indicators in wavelet and curvature analysis. Sadhana, 31(4): 463-486, 2006.

Qiao P., Lu K., Lestari W., and Wang J. Curvature mode shape-based damage detection in composite laminated plates. Composite Structures, 80(3): 409–428, 2007.

Ratcliffe C. P. Damage detection using a modified Laplacian operator on mode shape data. Journal of Sound and Vibration, 204(3): 505-517, 1997.

Rucka M. and Wilde K. Crack identification using wavelets on experimental static deflection profiles. Engineering Structures, 28(2): 279-288, 2006.

Stubbs N., Kim J. T., and Topole K. An efficient and robust algorithm for damage localization in offshore platforms. In Proceedings of the ASCE Tenth Structures Congress, pages 543-546, 1992.

Wang J. and Qiao P. Improved Damage Detection for Beam-type structures using a Uniform Load Surface. Structural Health Monitoring, 6(2): 99-110, 2007.

Wang Q. and Deng X. Damage detection with spatial wavelets. International Journal of Solids and Structures, 36(23): 3443–3468, 1999.

Wu D. and Law S. S. Damage localization in plate structures from uniform load surface curvature. Journal of Sound and Vibration, 276(1-2): 227-244, 2004.

Yan Y. J., Cheng L., Wu Z. Y., and Yam L. H. Development in vibration-based structural damage detection technique. Mechanical Systems and Signal Processing, 21(5): 2198–2211, 2007.

Yoon M. K., Heider D., Gillespie J. W., Ratcliffe C. P., and Crane R. M. Local damage detection using the two-dimensional gapped smoothing method. Journal of Sound and Vibration, 279(1-2): 119-139, 2005.

Yoon M. K., Heider D., Gillespie J. W., Ratcliffe C. P., and Crane R. M. Local damage detection with the global fitting method using operating deflection shape data. J Nondestruct Eval., 29(1): 25-37, 2010.

Zhang Z. and Aktan A. E. Application of modal flexibility and its derivatives in structural identification. Research in Nondestructive Evaluation, 10(1): 43–61, 1998.